Dynamics of Fractal Cluster Gels with Embedded Active Colloids

Megan E. Szakasits, Wenxuan Zhang, and Michael J. Solomon
University of Michigan, Ann Arbor, Michigan 48109, USA
(Received 6 November 2016; published 31 July 2017)

We find that embedded active colloids increase the ensemble-averaged mean squared displacement of particles in otherwise passively fluctuating fractal cluster gels. The enhancement in dynamics occurs by a mechanism in which the active colloids contribute to the average dynamics both directly through their own active motion and indirectly through their excitation of neighboring passive colloids in the fractal network. Fractal cluster gels are synthesized by addition of magnesium chloride to an initially stable suspension of 1.0 μm polystyrene colloids in which a dilute concentration of platinum coated Janus colloids has been dispersed. The Janus colloids are thereby incorporated into the fractal network. We measure the ensemble-averaged mean squared displacement of all colloids in the gel before and after the addition of hydrogen peroxide, a fuel that drives diffusiophoretic motion of the Janus particles. The gel mean squared displacement increases by up to a factor of 3 for an active to passive particle ratio of 1:20 and inputted active energy—defined based on the hydrogen peroxide's effect on colloid swim speed and run length—that is up to 9.5 times thermal energy, on a per particle basis. We model the enhancement in gel particle dynamics as the sum of a direct contribution from the displacement of the Janus particles themselves and an indirect contribution from the strain field that the active colloids induce in the surrounding passive particles.

DOI: 10.1103/PhysRevLett.119.058001

Colloidal gels are a class of disordered solids that transition from fluidlike to solidlike behavior as a function of the strength and range of the interparticle attraction and colloid volume fraction. Their slow dynamics arise due to attractive potential interactions that bond particles into a network [1,2]. Diffusion-limited cluster aggregation (DLCA) gels with fractal cluster structure are a well-understood limiting case of disordered gels [1]. Because of the mechanism of aggregation, which corresponds to spinodal decomposition, DLCA gels adopt a fractal cluster microstructure [3]. Investigating the relationships among microstructure, dynamics, and rheology of colloidal gels improves understanding of the relationship between phase equilibrium and dynamical retardation. Furthermore, colloidal gels display finite elasticity at low frequency and a yield stress; controlling these properties is important to industrial applications of gels, including in food, ceramic, pharmaceutical, agricultural, and consumer products [4–6].

Embedding active particles into colloidal gels is a potential route to affect their structure, dynamics, and mechanical properties. At a single-particle level, activity leads to self-propulsion [7], which can be generated by chemical reactions, light, or electric fields [8–10]. Activity can produce crystalline structures through dynamic self-assembly [11,12] or alter equilibrium structures [13,14]. Using active colloids to alter the dynamics of disordered and/or nonergodic media—such as gels—has received little attention. Activity has been investigated in cross-linked gel networks made with actin filaments [15,16], a disordered structure. In these materials, adenosine triphosphate-driven molecular motors activate actin, which increases the gel shear modulus [15]. There has been recent interest in the effect of activity on phase separation [17] and the glass transition [18]. Here we select fractal cluster gels as a model disordered, nonergodic material to study the effects of introduced active motion.

The structure of fractal cluster gels has been reported to follow $g(r) = (c/a^{d_f}) r^{d_f-3} \exp[-(r/R_c)^{\gamma}]$ for $r > 4a$ where $g(r)$ is the radial distribution function, c is a prefactor set by the density of particles within a cluster, a is the particle radius, d_f is the fractal dimension, R_c is the average cluster size, and γ is the cutoff exponent [19]. For $r < 4a$, short-range effects lead to specimen specific, nonfractal scaling [19]. The average cluster size, R_c, is $R_c = a\phi_0^{d_f-3}$, where ϕ_0 is the particle volume fraction. A fractal dimension $d_f = 1.8$ is typical for DLCA gels. The low-frequency elastic modulus is $G_0 = \kappa_0 a^{\beta} R_c^{-1-\beta}$, where κ_0 is the bond stiffness and β is the elasticity exponent [20]. The microscale dynamics of particles in passive fractal cluster gels is related to their elastic modulus by $\lim_{t\to\infty}\langle x^2(t)\rangle = (k_bT/\pi R_c G_0)$, where $\langle x^2(t)\rangle$ is the ensemble-averaged mean squared displacement of particles within the gel. The dynamics of particles within the (passive) gel network are inversely proportional to the elasticity.

Here we show that the dynamics of a gel particle network are significantly affected when active motion is imparted to a dilute fraction of colloids. We embed Janus particles that are activated by hydrogen peroxide into fractal cluster gels and find that the mobility of the gel network increases with the additional Janus particle activity. This increase is generated by the sum of a direct contribution of the active particles to the gel dynamics and an indirect contribution in which the active particles enhance dynamics of surrounding

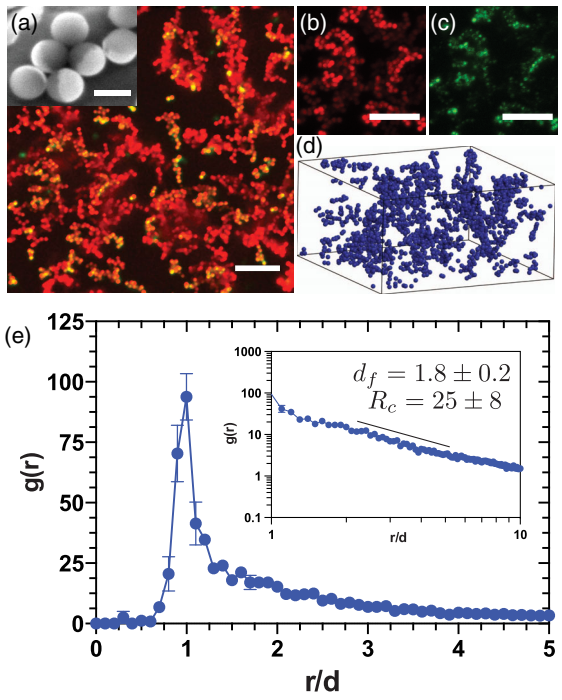

FIG. 1. (A) Three-dimensional projection of fractal cluster gel embedded with Janus particles with scanning electron microscopy image inset (scale bar 1 μm), (B) fluorescent and (C) reflective channels, scale bar (A)–(C) 10 μm. (D) Rendering of gel produced from three-dimensional image analysis. (E) Radial distribution function with fractal dimension and average cluster size inset (R_c is 25 μm).

passive particles due to their mutual connectivity in the fractal cluster network.

Fractal cluster gels are produced with 1.0 μm diameter polystyrene microspheres. Active particles are fabricated from the same microspheres by depositing 20 nm of platinum on one hemisphere of the particle [scanning electron microscopy, Fig. 1(a)]. Gelation is induced through addition of 16 mM divalent salt, magnesium chloride, to an initially stable suspension of Janus and polystyrene colloids [21]. The volume fraction of colloids used was 0.5%, and the ratio of Janus to polystyrene colloids was varied between 1:20 and 1:8. The elastic modulus of the gel network was measured to be 0.03 ± 0.01 Pa (Supplemental Material [22] Fig. 2), in agreement with the value predicted by a theory of fractal cluster microrheology ($G_{0\sim}0.01$ Pa [20]) Gels were visualized with confocal laser scanning microscopy (CLSM; Nikon A1Rsi, 100X objective, NA = 1.40); fluorescence and reflection channels imaged the stained polystyrene and reflective metal regions of the Janus particles, respectively [32]. Figures 1(a)–1(c) shows representative two-dimensional CLSM micrographs of fluorescent polystyrene particles [1(b)], reflective platinum [1(c)], and a merged image of the gel structure [1(a)]. H_2O_2 is delivered uniformly to the gel through a porous hydrogel membrane (cf., Supplemental Material [22]). We vary the concentration of H_2O_2 within the gel from 1.0–8 wt.% and image the gel 20 minutes after its addition. The H_2O_2 concentration range avoids the effects of oxygen bubbles produced by the H_2O_2 reaction, which are easily observed and can disrupt the gel.

From three-dimensional particle positions, we compute the radial distribution function, $g(r)$, and find d_f and R_c to be 1.8 ± 0.2 and 25 ± 8 μm [16]. We determine the active to passive particle ratio by analyzing three-dimensional image volumes obtained from the fluorescence and reflection channels individually, $X_{\text{active}} = (N_{\text{active}}/N_{\text{passive}} + N_{\text{active}}) = (N_{\text{reflection}}/N_{\text{fluorescence}})$. We find that the Janus particle concentration is highest closest to the coverslip and decreases further into the sample, Supplemental Material [22] Figs. 3(a) and 3(b), consistent with some sedimentation during the $MgCl_2$ gelation process, which embeds the Janus particles in the gel. Time series measurements taken at 5, 10, and 15 microns above the coverslip confirmed that the variation in Janus particle concentration does not affect gel dynamics, Supplemental Material Fig. 3(c). Results reported here were acquired 10 μm above the coverslip.

The mean squared displacement (MSD) of particles in a gel network with embedded Janus particles increases after the Janus particles are activated by H_2O_2. This enhancement

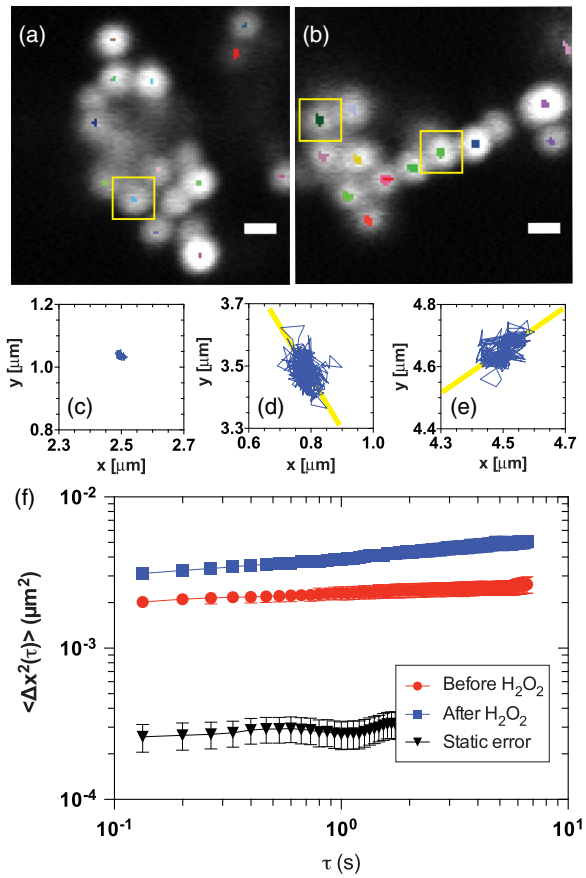

FIG. 2. (A) Trajectory of passive gel. (B) Trajectory of active gel. (C) Single particle dynamics of a passive gel trajectory. [(D) and (E)] Single particle dynamics in two active gel trajectories, with local orientation of cluster plotted as an overlaid line. (F) Ensemble-averaged MSD of gel before and after addition of 6.7% hydrogen peroxide.

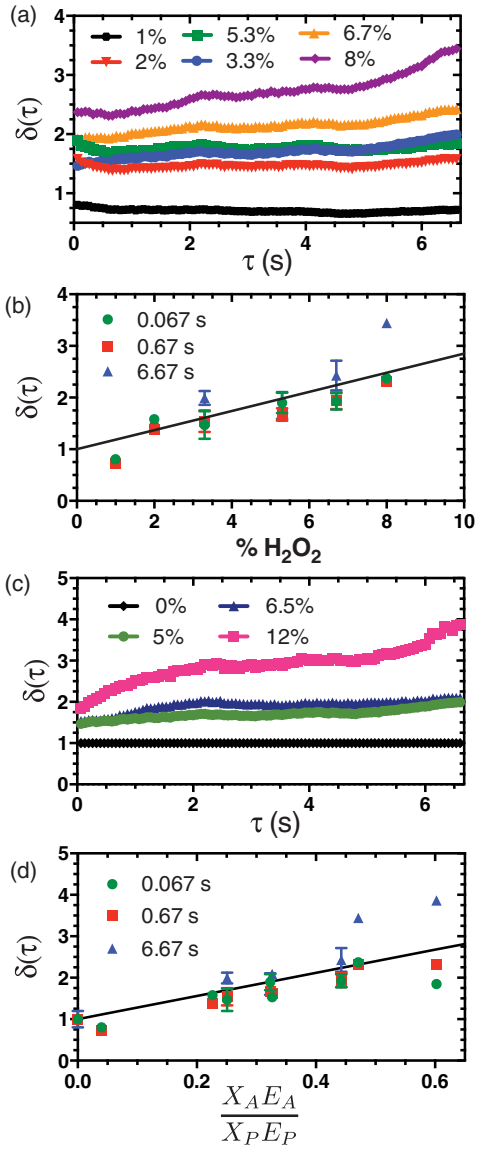

FIG. 3. Active gel ensemble-averaged dynamics. (A) MSD enhancement at a fixed active to passive particle ratio of 0.05 varying the hydrogen peroxide concentration. (B) $\delta(\tau)$ values at lag times 0.067, 0.67, and 6.67 s as a function of the hydrogen peroxide concentration at a fixed active to passive particle ratio of 0.05. (C) MSD enhancement at a fixed hydrogen peroxide concentration of 3.3% varying the ratio of active to passive particles. (D) $\delta(\tau)$ values at lag times 0.067, 0.67, and 6.67 s at each hydrogen peroxide and active particle concentration.

is apparent by comparing the trajectories of particles in Fig. 2(c) [from the indicated region of interest (ROI) in passive gel, Fig. 2(a)] and Figs. 2(d) and 2(e) [from ROIs in active gel, Fig 2(b)]. These data were acquired at a fixed active to passive colloid ratio of 0.05 with 6.7% H_2O_2. Figures 2(d) and 2(e) show that the displacement of the particular particles identified in the two ROI is aligned in a direction parallel to the orientation of the local colloidal cluster or filament; however, a more general analysis of $N = 78$ particles in different clusters finds that the particle dynamics tend to be aligned perpendicular to the local cluster orientation (cf., Supplemental Material [22]). When the dynamics of all particles are averaged, the MSD is isotropic, because the fractal cluster structure itself is isotropic.

We compute the ensemble-averaged MSD before and after the addition of H_2O_2, shown in Fig. 2(f), and find a significant increase in the MSD after H_2O_2 addition. Gels—both before and after H_2O_2 addition—display MSD curves that are nearly independent of time, with $\langle x^2(t)\rangle$ increasing as a power law with a small exponent of ~0.15; this behavior is consistent with prior literature [33] and indicates that nearly all colloids—active and passive—are localized within the gel network and the role of large-scale structural rearrangements is weak. Deviations from the ideal plateau dynamics could have multiple origins, including slow syneresis [34], arrested phase separation [35], or thermal expansion [36].

A kinetic study showed that the gels slowly age over the period of the measurements (Supplemental Material [22] Fig. 4) and in Fig. 2(f) there is a delay of 30 minutes between measurement of the passive gel dynamics and the active gel dynamics, to allow H_2O_2 diffusion. However, the change in gel MSD due to aging over a comparable 30-minute period is never more than 20%, which is much less than the change in dynamics due to H_2O_2 addition. The results of Fig. 2(f) can also be compared to the control experiment in which the same concentration of H_2O_2 is delivered to a gel comprised of just passive particles. In this case, the average MSD drops by the small percentage of ~30%. Evidently, the H_2O_2, a strong oxidizer, modulates the bond strength of passive particles in the gel to a small degree, in addition to its role in active motion. This effect was found to be, within error, independent of concentration (Supplemental Material [22] Fig 5) and in the opposite direction of the change when active particles were present. To account for this and plot only the effect of active motion, we report a measure $\delta(\tau)$ of the enhanced dynamics due to activity, computed as

$$\delta(\tau) = \frac{\langle x^2(\tau)\rangle_{\mathrm{H_2O_2,Janus}}\langle x^2(\tau)\rangle_{\mathrm{NoH_2O_2,Passive}}}{\langle x^2(\tau)\rangle_{\mathrm{NoH_2O_2,Janus}}\langle x^2(\tau)\rangle_{\mathrm{H_2O_2,Passive}}}. \quad (1)$$

The MSD enhancement, $\delta(\tau)$, describes the ratio of the ensemble-averaged MSD of the active and passive gels, corrected by the effect that adding H_2O_2 has on the passive gel.

$\delta(\tau)$ increases with increasing H_2O_2 concentration at a fixed active to passive particle ratio of 0.05 [Fig. 3(a)]. The enhancement is approximately independent of time and increases linearly as a function of the H_2O_2 concentration, Fig. 3(b). By embedding 5% active particles within the gel, the dynamics of all particles—both passive and active together—are enhanced by up to a factor of 3. Both the number of active colloids and the H_2O_2 concentration affect activity. Varying the ratio of active to passive colloids from 1:20 to 1:8 [Fig. 3(c)] increases $\delta(\tau)$. By increasing the number of active particles within the gel, we observe an increase in the gel mobility of up to about four times greater than passive gels.

While passive gel dynamics are driven by thermal energy, active gels are driven by energy inputted into the system by the catalytic oxidation of H_2O_2. Following Takatori *et al.*, the active energy of a particle, E_A, is given by $\xi V l$, where ξ is the hydrodynamic drag coefficient, V is the active particle's run velocity in free solution, and l is the active particle run length, equivalent to $l = \tau_R V$ where τ_R is the Brownian reorientation time, $\tau_R = (8\pi\mu a^3/k_B T)$ [37]. The free particle velocity is determined by fitting the MSD of the active colloids at each H_2O_2 concentration to $\Delta x^2 = 4D\Delta t + V^2\Delta t^2$, the limiting form of the active particle MSD at short times [7]. Results for each H_2O_2 concentration are in Supplemental Material Table I. Over the range of H_2O_2 concentrations studied, the activity imparted generates energies on a per particle basis that are 4.5–9.4 times greater than thermal energy. The ratio of active to passive energy in the gel is then $(X_{\text{active}}E_{\text{active}}/X_{\text{passive}}E_{\text{passive}}) = (X_{\text{active}}\xi V\tau_R/X_{\text{passive}}k_B T)$. Using this scaling, the effects of active particle number and H_2O_2 concentration collapse onto one curve, Fig. 3(d).

We present a simple model for the enhancement in gel dynamics induced by the embedded active particles. The model resolves the active particle's effect into direct and indirect contributions. Each active particle directly contributes a relative enhancement of $E_{\text{active}}/k_B T$ to the gel dynamics. The active particles also contribute indirectly to the MSD enhancement by inducing a strain field on the surrounding passive particles in the fractal cluster, which is the response of the surrounding passive particles to the active motion. This indirect contribution is modeled by assuming that the fractal cluster gel is a linearly elastic medium. The deformation field, $\mathbf{u}(\mathbf{x})$, induced by the displacement of the active particle in the gel is

$$\mathbf{u}(\mathbf{x}) = \frac{3a}{10-12\nu}\left[\left(\frac{3-4\nu}{r}+\frac{a^2}{3r^3}\right)\mathbf{U}+\left(1-\frac{a^2}{r^2}\right)\frac{\mathbf{U}\cdot\mathbf{x}\mathbf{x}}{r^3}\right], \tag{2}$$

where r is the radial distance, v is the Poisson ratio, a is the particle radius, $\mathbf{U}$ is the active particle displacement, and $\mathbf{x}$ is the particle position [6]. This induced strain field, plotted in Fig. 4(a), is anisotropic and long range. We use a value of $\nu = 0.5$ and show effects of varying ν in Supplemental Material [22] Table II.

The predicted direct contribution of the active particles to the MSD can be compared to measurements of the localization of Janus particles in the gel by reflection CLSM of the platinum layers [Fig. 1(c)]. We compute $\delta(\tau)$ for the embedded Janus particles with 6.7% H_2O_2. At long times, $\delta(\tau) \sim 7$, the enhancement is significantly greater than for the passive particles, $\delta_{\text{Passive}} \sim 2.5$, and comparable to the active energy, $\frac{E_{\text{Active}}}{k_B T} = 9.0$ predicted from single-particle measurements [Fig. 4(b) and Supplemental Material [22] Table I]. By summing the passive, direct, and indirect contributions, the MSD enhancement of the active gel is

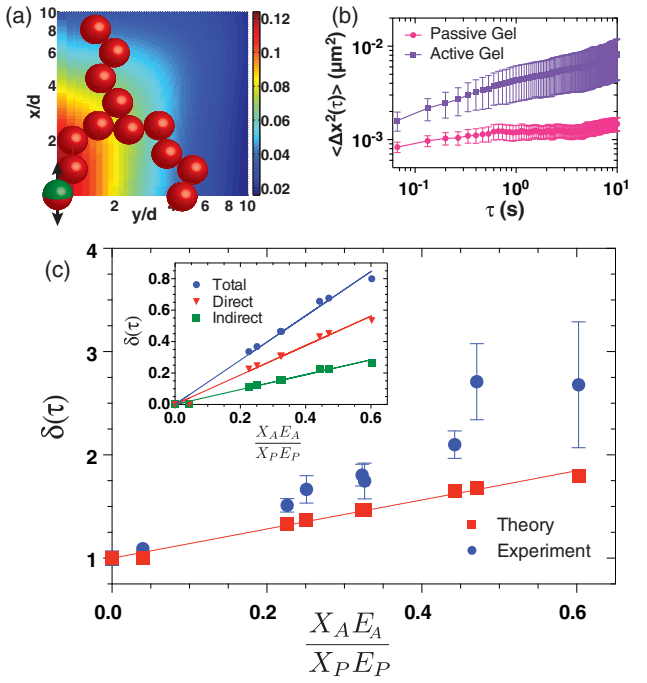

FIG. 4. (A) Strain field induced on the gel network by displacement of the active particle for active to passive particle ratio 0.05 and 6.7% H_2O_2, where U_x is 0.2 μm. The color bar shows magnitude of the strain field in microns. (B) MSD of Janus particle in gel network before and after addition of 6.7% H_2O_2. (C) Comparison of experimental MSD enhancement to predicted values, with total enhancement, direct and indirect contributions inset. Theory values were calculated pointwise at each experimental condition using parameters measured for free active particles. Lines for theory are to guide the eye.

$$\delta(t) = 1 + X_{\text{active}}\left(\frac{E_{\text{active}}}{k_B T} + X_{\text{passive}}\int_{2a}^{R_c} 4\pi r^2 dr \times \int_0^{\pi}\sin\theta d\theta\int_0^{2\pi} g(r)\langle u(r,\theta,\phi)^2\rangle d\phi\right). \tag{3}$$

The first term (unity) accounts for the passive motion. The second term includes the two effects of activity—the direct and indirect contributions. The indirect contribution from the induced strain field is calculated by integrating over the anisotropic strain field [Eq. (2)] induced in a gel with an isotropic fractal structure given by $g(r)$. We use the experimentally measured $g(r)$ for $r < 4a$ and the fractal cluster model for $r > 4a$ [19] (cf., Supplemental Material [22]). We compute the MSD enhancement from the direct (δ_{direct}) and indirect (δ_{indirect}) contributions, plotted in the inset of 4(c). The integration of the right-hand term is carried out to the cluster radius, consistent with other microrheology models of fractal gels [20,38]; however, the particular choice of R_c is not critical, because $g(r)$ is low for $r > R_c$ (cf., Supplemental Material [22]).

Although smaller than the direct contribution, the indirect contribution to the active gel MSD is still significant [cf., Fig. 4(c)]. The theory underpredicts the MSD

enhancement, particularly at high H_2O_2 concentrations. Reasons for the model underestimation might be (i) nonideal experimental conditions, such as an inhomogeneous concentration of Janus particles in the gel, (ii) interactions among the strain fields induced by neighboring Janus particles, (iii) reflections of induced deformations of surrounding passive particles back onto the active particle excitation, (iv) deviations of the fractal cluster structure elastic response from that of a homogeneous elastic medium, and (v) the model's inclusion of only intracluster effects, consistent with the strong-link regime of fractal cluster models [20,38]. Future work addressing points (iv) and (v) could yield a higher fidelity description of the strain field induced by active Janus particles in the fractal cluster gel.

Active particles embedded within a fractal gel network increase the average mobility of particles in the gel. The amount of dynamical enhancement collapses onto a single curve when the energy that an active particle contributes to the gel is determined by the swim pressure [37]. $\delta(\tau)$ increases linearly with $X_A E_A / X_P E_P$ over the parameter range studied; $\delta(\tau)$ is predicted with some underestimation when direct and indirect contributions of the active particles to the gel dynamics are modeled. Here we focused on the microdynamical changes induced in a gel with embedded activity; having found they are significant, future work might analyze how the activity affects other microdynamical changes, such as the correlated two-dimensional displacement field generated around an active particle by its fluctuations and the macroscopic rheological properties of the elastic fractal cluster gel. Effects that could be observable include a change in the gel elastic modulus, as well as swelling of the gel induced by the active particles embedded within it [39].

We acknowledge discussion with J. F. Brady about the active particle energy and T. F. Scott about the photoinitiator. This work is supported by NSF Grant No. CBET 1232937. M. E. S. acknowledges support by a Rackham Merit Fellowship. This work was performed in part at the University of Michigan Lurie Nanofabrication Facility.

[1] V. Prasad, V. Trappe, A. D. Dinsmore, P. N. Segre, L. Cipelletti, and D. A. Weitz, Faraday Discuss. **123**, 1 (2003).
[2] E. Zaccarelli, J. Phys. Condens. Matter **19**, 323101 (2007).
[3] M. Carpineti and M. Giglio, Phys. Rev. Lett. **68**, 3327 (1992).
[4] R. Mezzenga, P. Schurtenberger, A. Burbidge, and M. Michel, Nat. Mater. **4**, 729 (2005).
[5] L. C. Hsiao, R. S. Newman, S. C. Glotzer, and M. J. Solomon, Proc. Natl. Acad. Sci. U.S.A. **109**, 16029 (2012).
[6] M. H. Lee and E. M. Furst, Phys. Rev. E **77**, 041408 (2008).
[7] J. R. Howse, R. A. L. Jones, A. J. Ryan, T. Gough, R. Vafabakhsh, and R. Golestanian, Phys. Rev. Lett. **99**, 048102 (2007).
[8] S. Sánchez, L. Soler, and J. Katuri, Angew. Chem., Int. Ed. Engl. **54**, 1414 (2015).
[9] S. J. Ebbens and J. R. Howse, Soft Matter **6**, 726 (2010).
[10] W. F. Paxton, S. Sundararajan, T. E. Mallouk, and A. Sen, Angew. Chem., Int. Ed. Engl. **45**, 5420 (2006).
[11] J. Palacci, S. Sacanna, A. P. Steinberg, D. J. Pine, and P. M. Chaikin, Science **339**, 936 (2013).
[12] N. H. P. Nguyen, D. Klotsa, M. Engel, and S. C. Glotzer, Phys. Rev. Lett. **112**, 075701 (2014).
[13] S. McCandlish, A. Baskaran, and M. Hagan, Soft Matter **8**, 2527 (2012).
[14] B. van der Meer, L. Filion, and M. Dijkstra, Soft Matter **12**, 3406 (2016).
[15] T. B. Liverpool, M. C. Marchetti, J.-F. Joanny, and J. Prost, Europhys. Lett. **85**, 18007 (2009).
[16] D. Mizuno, C. Tardin, C. F. Schmidt, and F. C. MacKintosh, Science **315**, 370 (2007).
[17] I. Buttinoni, J. Bialké, F. Kümmel, H. Löwen, C. Bechinger, and T. Speck, Phys. Rev. Lett. **110**, 238301 (2013).
[18] A. Yazdi and M. Sperl, Phys. Rev. E **94**, 032602 (2016).
[19] M. Lattuada, H. Wu, and M. Morbidelli, J. Colloid Interface Sci. **268**, 106 (2003).
[20] A. H. Krall and D. A. Weitz, Phys. Rev. Lett. **80**, 778 (1998).
[21] G. Yin, Doctoral thesis, University of Michigan 2007.
[22] See Supplemental Material http://link.aps.org/supplemental/10.1103/PhysRevLett.119.058001, which includes Refs. [23–31].
[23] T. Majima, W. Schnabel, and W. Weber, Macromol. Chem. Phys. **192**, 2307 (1991).
[24] J. Scrimgeour, J. K. Cho, V. Breedveld, and J. Curtis, Soft Matter **7**, 4762 (2011).
[25] L. C. Hsiao, B. A. Schultz, J. Glaser, M. Engel, M. E. Szakasits, S. C. Glotzer, and M. J. Solomon, Nat. Commun. **6**, 8507 (2015).
[26] D. Allan, T. A. Caswell, N. Keim, F. Boulogne, R. W. Perry, and L. Uieda, trackpy: Trackpy v0.2.4, 2014, DOI: 10.5281/zenodo.12255.
[27] J. Crocker and D. Grier, J. Colloid Interface Sci. **179**, 298 (1996).
[28] T. Savin and P. S. Doyle, Biophys. J. **88**, 623 (2005).
[29] J. Schindelin, I. Arganda-Carreras, E. Frise, V. Kaynig, M. Longair, T. Pietzsch, S. Preibisch, C. Rueden, S. Saalfeld, B. Schmid, J.-Y. Tinevez, D. J. White, V. Hartenstein, K. Eliceiri, P. Tomancak, and A. Cardona, Nat. Methods **9**, 676 (2012).
[30] Y. Gong, PhD thesis, MOSAIC Group, ETH Zurich, 2015.
[31] R. H. Pritchard, P. Lava, D. Debruyne, and E. M. Terentjev, Soft Matter **9**, 6037 (2013).
[32] A. A. Shah, B. Schultz, K. L. Kohlstedt, S. C. Glotzer, and M. J. Solomon, Langmuir **29**, 4688 (2013).
[33] C. J. Dibble, M. Kogan, and M. J. Solomon, Phys. Rev. E **74**, 041403 (2006).
[34] L. Cipelletti, S. Manley, R. C. Ball, and D. A. Weitz, Phys. Rev. Lett. **84**, 2275 (2000).
[35] P. J. Lu, E. Zaccarelli, F. Ciulla, A. B. Schofield, F. Sciortino, and D. A. Weitz, Nature (London) **453**, 499 (2008).
[36] S. Mazoyer, L. Cipelletti, and L. Ramos, Phys. Rev. Lett. **97**, 238301 (2006).
[37] S. C. Takatori, W. Yan, and J. F. Brady, Phys. Rev. Lett. **113**, 028103 (2014).
[38] W.-H. Shih, W. Y. Shih, S.-I. Kim, J. Liu, and I. A. Aksay, Phys. Rev. A **42**, 4772 (1990).
[39] S. C. Takatori and J. F. Brady, Soft Matter **10**, 9433 (2014).